magnetochemistry

MDPI

Article

Structural Parameters of the Interaction between Ciprofloxacin and Human Topoisomerase-II β Enzyme: Toward New ^{19}F NMR Chemical Shift Probes

Thais Aparecida Sales [1], Mateus Aquino Gonçalves [1] and Teodorico Castro Ramalho [1,2,*]

[1] Department of Chemistry, Federal University of Lavras, Lavras CEP 37203-202, Brazil
[2] Department of Chemistry, Faculty of Science, University of Hradec Králové, 500 03 Hradec Králové, Czech Republic
* Correspondence: teo@ufla.br

Abstract: New tools for cancer diagnosis are being studied since early diagnosis can be crucial for a successful treatment. In this context, the use of NMR probes constitutes an efficient method of diagnosis. In this study, we investigated the use of ciprofloxacin to indirectly label the overexpression of topoisomerase-II enzymes by changes in ^{19}F NMR chemical shifts of ciprofloxacin. Increased topoisomerase-II expression has been associated with cancer occurrence, mainly with aggressive forms of breast cancer, thus constituting a promising molecular target for new tumor cell identifiers. Using DFT calculations, we performed a spectroscopy analysis of ciprofloxacin in different chemical environments and evaluated the solvent and enzymatic effects. Our results show that ciprofloxacin forms a stable complex with the enzyme, and the main intermolecular interactions between ciprofloxacin and human topoisomerase-IIβ are hydrogen bonds, followed by π-π stacking and electrostatic interactions. Additionally, a shift of 6.04 ppm occurs in the ^{19}F NMR signal when ciprofloxacin interacts with the human topoisomerase-IIβ enzyme, and this parameter may be an indirect marker indicating the overexpression of these enzymes in the body.

Keywords: spectroscopic probe; computational methods; drug repositioning; cancer diagnosis

Citation: Sales, T.A.; Gonçalves, M.A.; Ramalho, T.C. Structural Parameters of the Interaction between Ciprofloxacin and Human Topoisomerase-II β Enzyme: Toward New ^{19}F NMR Chemical Shift Probes. *Magnetochemistry* **2022**, *8*, 181. https://doi.org/10.3390/magnetochemistry8120181

Academic Editor: Serge Smirnov

Received: 26 October 2022
Accepted: 29 November 2022
Published: 7 December 2022

1. Introduction

Fluoroquinolones (FQ), introduced more than 20 years ago, are a quinolone derivative class of molecules known for their antibacterial activity [1]. The broad-spectrum commercialized antibacterial agent ciprofloxacin (CPX) is representative of the FQs [2–4]. These compounds exert antibacterial activity through the inhibition of two bacterial enzymes: DNA gyrase and topoisomerase II [5,6]. The latter is considered to be the primary target of several anticancer agents, such as doxorubicin and etoposide [7–9]. Researchers continue to investigate the development of new anticancer drugs based on evidence indicating increased levels of topoisomerase II in several types of proliferating cancer cells, including gallbladder cancer [10], aggressive breast cancer [10–12], epithelial ovarian cancer [10,13–15], lymphomas and sarcomas [16–18], and colon cancer [10]. Increased levels of this enzyme associated with aggressive breast cancer are related to increased expression of the oncogene HER2 neu, predicted disease-related death, lymph node metastasis, and advanced tumor stage [19].

Currently, cancer is one of the deadliest diseases in the world [20–23], and one factor that contributes to numerous deaths is the difficulty in diagnosis [24,25]. An early diagnosis can be influenced by three main factors: awareness of search for healthcare, clinical and diagnostic evaluation, and access to treatment [26]. Regarding the latter, it is important to stress that access barriers are mainly a problem in underdeveloped countries. In developed countries, a prognosis is reached in more than 70% of cases, while in underdeveloped countries only 20–50% of patients receive an early diagnosis, which compromises the

chance of a cure [27]. In this sense, the research, development, and implementation of fast, simple, and low-cost tools can help change this reality [28–30]. New research into diagnostic tools is aimed at developing systems that are increasingly capable of locating species in different environments, with high specificity and resolution [28,31–34]. For this purpose, many spectroscopic techniques have been explored, such as nuclear magnetic resonance (NMR) [29,35–42]. Molecules that interact with key enzymes can act as spectroscopic probes [43]. These molecules are of great interest due to their high sensitivity and ease of operation, enabling rapid location within live systems [44].

In CPX molecules, the presence of a fluorine atom allows the application of ^{19}F NMR spectroscopy techniques. The large chemical shift range, together with the high sensitivity of ^{19}F NMR nuclei, makes the use of ^{19}F NMR an extremely attractive proposition [45]. Additionally, considering the scarcity of naturally occurring fluorine compounds, ^{19}F NMR offers an attractive option for investigating the interactions between proteins and other biomolecules, as well as the structure and mechanisms of action of fluorinated inhibitors [46]. Moreover, another advantage of ^{19}F NMR is that this technique is particularly useful for studying large proteins that cannot be easily probed by conventional NMR experiments [47].

Computational methods have been widely employed to predict the spectroscopic properties of different compounds for various purposes [48–50]. Theoretical methods offer a fast, efficient and practical way to investigate changes in the NMR properties of different compounds, which can be caused by several factors, such as changes in the chemical environment or structure of the molecule that can occur due to interactions with biological macromolecules [29,51]. In that context, the aim of this study is to theoretically investigate the behavior of CPX in the human topoisomerase-II β (hTOPO-II) active site, evaluating how this interaction affects the ^{19}F NMR chemical shift of CPX to propose the use of CPX as a spectroscopic NMR probe for cancer diagnosis.

2. Methodology

2.1. Molecular Dynamics (MD) Simulations

The theoretical analysis in this study was performed with the DNA topoisomerase II β enzyme. FQs are known inhibitors of both DNA gyrase and topoisomerase. However, considering our proposal to use this drug as an NMR probe in humans, we have determined that there is no need for a study on the interaction of ciprofloxacin with DNA gyrase since this enzyme is not present in large eukaryotes [8,52,53]. The first Molecualr Dynamics (MD) simulation was performed with CPX in the active site of the hTOPO-II enzyme. For the simulation, the crystallographic structure of hTOPO-II in complex with DNA (PDB-ID 5ZAD) was obtained from Protein Data Bank [54] while CPX topology and charge data were sourced from the Automated Topology Builder (ATB) Repository [55]. The simulation was performed by employing the GROMACS® Package [56] using the Gromos 54a7 force field [57]. The system CPX:hTOPO-IIβ was solvated inside a cubic box with the SPC water model. A steepest descent algorithm was employed for the minimization step, stopping minimization when the maximum force was under 10.0 kJ/mol. A heading step of 1 ps was performed in the NVT ensemble, and for equilibrium simulation in the NPT ensemble, the temperature and pressure, respectively, were controlled by the v-rescale thermostat (300 K) and Berendsen barostat (1 bar). The last simulation step was the performance of 10 ns of MD simulation using the Parrinello-Rahman barostat and v-rescale thermostat. Coordinates, velocities, and energies were saved at 10.0 ps of simulation, obtaining 1000 frames at the end of simulation. For both steps, the leap-frog integrator was adopted.

Finally, to select the best conformations, the optimal wavelet signal compression algorithm (OWSCA) [58] was used. This algorithm is based on a wavelet compression strategy, in which an optimization algorithm is applied to compress the maximum number of wavelet coefficients, instead of using heuristically chosen parameters. A second MD simulation of free CPX in a water box (CPX:explicit water system) was also performed under the same conditions mentioned above for comparison of ^{19}FNMR chemical shifts.

2.2. ^{19}F NMR Chemical Shift (δ) Calculations

All ^{19}F NMR shielding constant calculations of this step were performed using the GAUSSIAN 09 software package [59] at the DFT level, with the B3LYP functional and Dunning basis set [60] with diffuse function [61,62] aug-cc-pVDZ, and by applying the gauge-including atomic orbital (GIAO) method [63]. These levels of theory were selected based on previous parametrization studies performed on NMR calculations [64] for the CPX molecule [49]. Calculations were made for CPX in the selected frames of two MD systems using the ONIOM model [65]. In the CPX:explicit water system, the first solvation shell was maintained, and the obtained values were compared with the results obtained for the CPX:hTOPO-II system. Additionally, ^{19}F NMR shielding constants were calculated for CPX in a vacuum (CPX:vacuum) and, using the IEF-PCM solvation model [66], when employing water as solvent (CPX: implicit water). For both systems, the initial structures were generated from a conformational analysis in Spartan 14® software using molecular mechanics. After this step, the ten lowest energy conformations obtained were subjected to geometry optimization calculations in Gaussian software at the B3LYP/aug-cc-pVDZ level of theory. Then, NMR calculations were performed in the same way as in the previous systems.

The theoretical ^{19}F NMR chemical shifts were calculated in ppm according to Equation (1) [64]. The chemical shifts were expressed relative to the external chemical shift reference CF_3COOH. Theoretical results obtained were compared with experimental data, where measurements were carried out using the same reference compound [67,68].

$$\delta_{teor} = \sigma_{ref}^{cal} - \sigma_{CPX}^{cal} \quad (1)$$

where σ_{ref}^{cal} and σ_{CPX}^{cal} are the isotropic NMR shieldings of the reference compound (CF_3COOH) and the CPX frame, respectively. To analyze the agreement between theoretical values for chemical shifts and the experimental ^{19}F NMR chemical shift data, the $\Delta\delta$ calculation was performed using Equation (2), as follows [64]:

$$\Delta\delta = \delta_{exp} - \delta^{cal} \quad (2)$$

3. Results and Discussion

It is well-known that CPX, like all FQs, is a bacterial topoisomerase inhibitor [6,69]. However, due to the presence of these enzymes in the human body, many experimental researches have been focused recently on the potential of this drug and its derivatives to inhibit human topoisomerases [12,70–76]. Theoretical investigations have already been conducted in order to better understand the mechanisms of action and the main differences between the interactions of TOPO-II in the two organisms [77,78]. A previous study that investigated the interaction of thirteen FQs with human topoisomerases using molecular docking techniques showed that CPX is able to form a hydrogen bond with the hTOPO-IIβ active site on the amino acid Asp 479 [79]. The study found that the binding affinity was -9.62 kcal·mol^{-1}. Another recent theoretical investigation explored how CPX binds to different sites of the hTOPO-IIβ enzyme [77]. Through molecular docking calculations, the authors showed that CPX has a similar interaction energy in both human and bacterial enzymes and that CPX preferentially interacts in the same locale as the chemotherapeutic agent etoposide. The study found that the interaction energy of CPX was -71.62 kcal·mol^{-1} and that CPX was able to form hydrogen bonds with Glu477, Tyr 821, Gln778, and Asp 479 amino acid residues.

All the studies referenced above utilized the molecular docking technique in their investigations. Molecular docking is an important computational technique in structural biology and computer-aided drug design [80]. The main goal of this type of computational simulation is to evaluate the most feasible binding geometries of a ligand to a target protein whose three-dimensional structure is known [81,82]. Despite their fundamental importance in this research field, docking studies only provide a static view of the interactions between the ligand and the protein. MD simulations, on the other hand, are used to analyze the

dynamic behavior of these interactions as well as of the entire system, helping to reproduce the biological events in a computer simulation [83,84]. Here, the main proposal is to investigate the possibility of using the well-known antibiotic ciprofloxacin as a ^{19}F NMR chemical shift probe to localize the overexpression of hTPO-IIβ, which is associated with cancer incidence [10,85]. For this, a dynamic analysis of the system is of crucial importance.

3.1. MD Simulations

In order to analyze the influence of the chemical environment on the conformational change of CPX, two MD simulations were performed. One simulation was carried out with CPX in the hTOPO-II active site (CPX:hTOPO-II system) and the other was performed with CPX only in a water box (CPX:explicit water). With the analysis of the root mean square deviation (RMSD) of CPX in both systems (Figure 1), it was possible to observe that the systems reached equilibrium at around 2000 ps of simulation, and this time was used as the starting time for the selection of representative frames using an OWSCA algorithm. As shown in Figure 1, there was a slightly higher flexibility of CPX in the aqueous system when compared to molecules in the enzyme active site. Once in the active site, the molecule has greater conformational restriction due to the presence of the surrounding amino acids, with which it engaged in intermolecular interactions. Additionally, the RMSD levels for CPX in the hTOPO-II active site were around 0.1 nm (1 Å), indicating high stability of the structures [86,87].

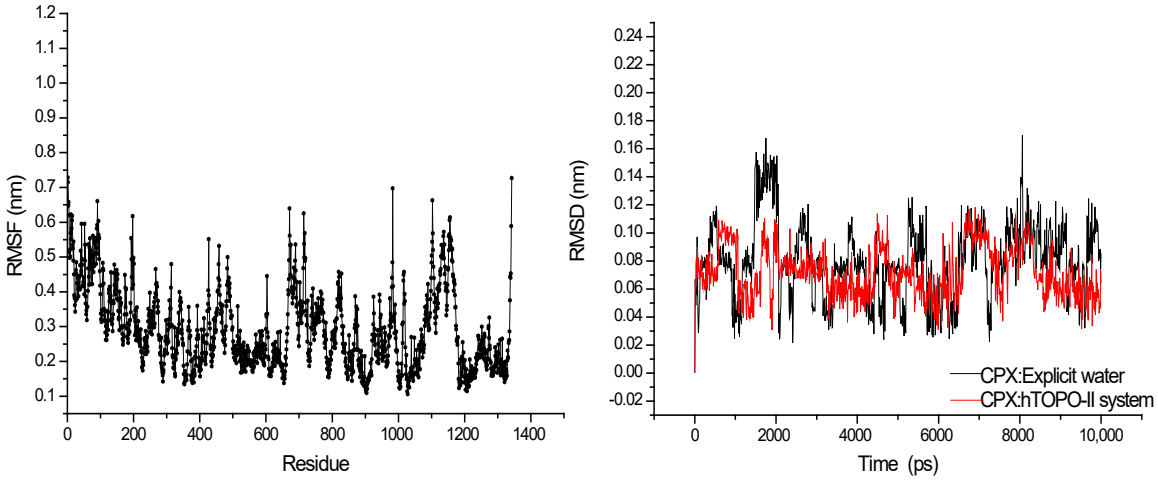

Figure 1. RMSF (left) and RMSD (right) for ciprofloxacin molecule inside the active site (CPX:hTOPO-II) and out of the active site of the topoisomerase-II enzyme (CPX: explicit water).

Figure 1 also shows the root mean square fluctuation (RMSF). Together with the RMSD, the relative RMSF provides information about the fluctuation of each residue in the simulation. Understanding the relationship between the flexibility of the residues and the interaction with the ligand facilitates the identification of regions with great flexibility. Generally, the flexibility of the terminal residue and surface loop regions is higher and the protein core is more limited [88]. As can be seen, the fluctuation of residues around 400–600 is more restricted than at other points, which may indicate that CPX forms a stable connection in this region. The total energy variation obtained for CPX in both systems, CPX:hTOPO-II and CPX:explicit water, is shown in Figure 2 (A and B). The values remained balanced over the course of the simulation, showing a stabilization of both systems. Regarding the ligand–protein interaction energy, also shown in Figure 2, in the CPX:hTOPO-II system, the average value of the total interaction energy was equal to -94.27 ± 1.02 kJ.mol^{-1}, which corresponds to the sum of the short-range electrostatic (coulombic) interactions, -36.27 ± 0.77 kJ·mol^{-1}, and the short-range Lennard-Jones interactions, whose average value was equal to -58 ± 0.67 kJ·mol^{-1}.

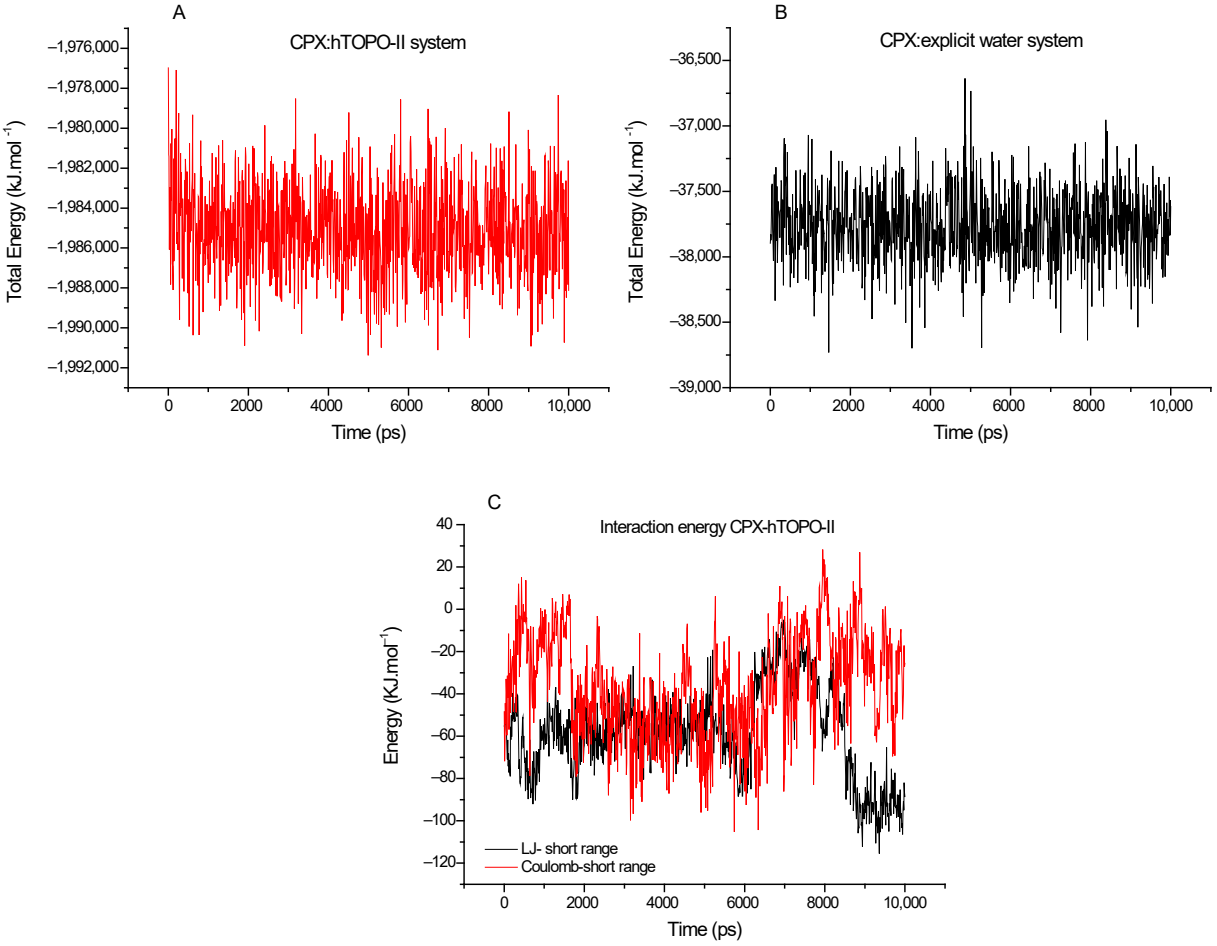

Figure 2. Energy graphs extracted from MD simulations. (**A**,**B**) Total energy variation for the CPX:hTOPO-II and CPX:explicit water systems, respectively. (**C**) Interaction energy graph for the CPX:hTOPO-II complex. In C, the black line corresponds to Coulombic-type interactions while the red line corresponds to Lennard-Jones-type interaction energy.

The hydrogen bonds formed between CPX and hTOPO-II β were the main interactions responsible for the stability of the molecule in the enzyme active site, as shown in Table 1. This details the main residues that participated in the intermolecular interactions for the representative conformations selected by the OWSCA algorithm. Additionally, the number of hydrogen bonds formed during the MD simulation for all frames is shown in Figure 3. By analyzing the figure, it can be observed that the CPX shows three hydrogen bonds with hTOPO-IIβ, two of which are quite frequent during most of the simulation time.

Table 1. Intermolecular interactions between human topoisomerase-II β enzyme and ciprofloxacin molecule during molecular dynamics simulation.

Frame	Time (ps)	Residue	Interaction Type
1	2000	Asn 520	HBond
2	2200	Asn 520	HBond
3	2300	Leu 507	HBond
4	2400	Asn 520	HBond
5	2600	Asn 520; Gln 516	HBond

Table 1. *Cont.*

Frame	Time (ps)	Residue	Interaction Type
6	3000	Asn 520	HBond
7	3100	Asn 520	HBond
8	3200	Glu 519; Asn 520; Ala 521	HBond
9	3700	Asn 520; Ala 521	HBond
10	3900	Asn 520; Ala 521	HBond
11	4200	Asn 520	HBond
12	4400	Asn 520; Ala 521	HBond
13	4700	Asn 520; Ala 521	HBond
14	5100	Asn 520; Ala 521	HBond
15	5500	Ala 521	HBond
16	7000	-	-
17	7300	Lys 505	π-π; Electrostatic HBond
18	7500	-	-
19	7700	Arg 503	HBond
20	7900	Arg 503; Lis 505; Gly 504	π-π
21	8000	-	-
22	8250	Lys 505	HBond; π-π
23	8800	-	-
24	9000	Ile 506	HBond
25	9200	Ile 506	HBond
26	9400	Ile 506	HBond
27	9500	-	
28	9800	Ile 506	HBond
29	10,000	Ile 506	HBond

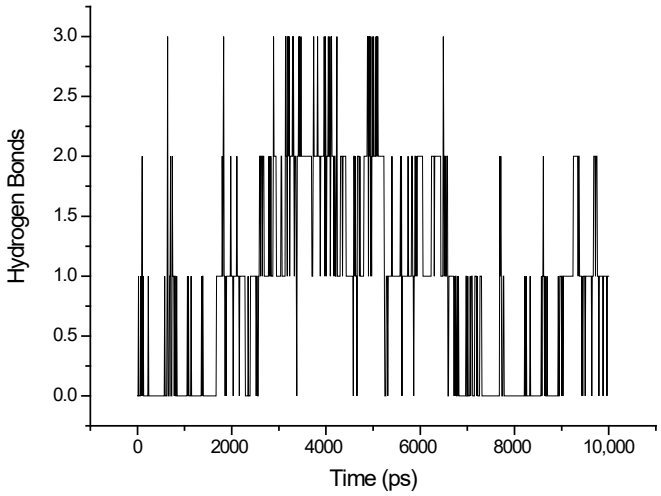

Figure 3. Hydrogen bonds formed between CPX and hTOPO-II β during the molecular dynamics simulation.

Figure 4A shows the hydrogen bonds formed for frame **8**, at 3200 ps of simulation, which is the point when the greatest number of hydrogen interactions can occur. The

residues that participate in the interaction are Glu 519, Asn 520, and Ala 521. Figure 4B also shows the π-π stacking interactions between CPX and amino acids residues Arg 503, Lis 505, and Gly 504.

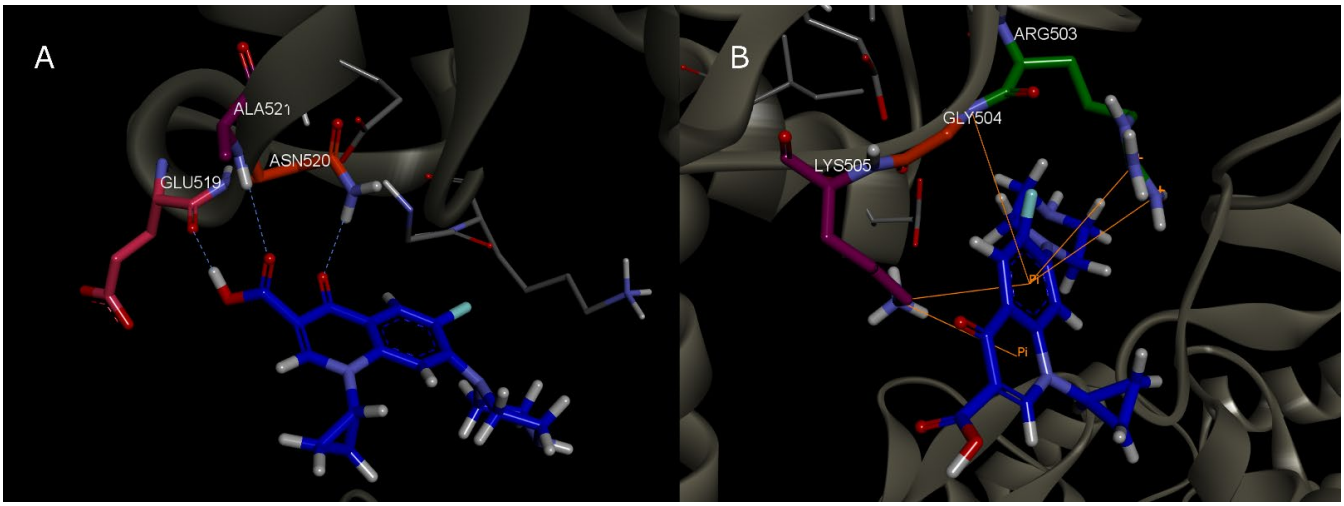

Figure 4. Intermolecular interactions during molecular dynamics simulation. (**A**) Hydrogen bonds formed between CPX and the amino acids Glu 519, Asn 520, and Ala 521 at 3200 ps of simulation. (**B**) π-π stacking interactions between CPX and amino acids Arg 503, Lis 505, and Glu 504 at 7900 ps of simulation.

In the next step, the chemical shift calculation was performed for the representative configurations in both systems. For the CPX:explicit water system, the first solvation shell was maintained in order to represent the presence of explicit solvent molecules in the NMR calculation. For the CPX:hTOPO-II system, amino acid residues participating in hydrogen interactions with CPX were maintained in order to represent the change in the chemical environment of the molecule inside the active site.

3.2. Spectroscopic Parameters: ^{19}F- Chemical Shifts (δ)

Fluorinated compounds have a wide range of applications, including anti-inflammatory drugs, anesthesiology, and cancer therapy. Di- and trifluoromethyl groups can considerably improve the profile of bioactive compounds by increasing their uptake and permeability as they exhibit unique properties such as high electronegativity, lipophilicity, and high steric demand [89]. ^{19}F NMR spectroscopy is a rapidly emerging tool and an attractive option for studies of new spectroscopic probes for biological use [90–93]. The main advantages include its high sensitivity, the very low background signal, the scarce natural occurrence of fluorinated compounds, and the high magnetic moment that results in a ^{19}F NMR sensitivity similar to that of ^{1}H [94]. The fluorinated compound chosen for this work is a widely marketed and prescribed antibiotic drug throughout the world [49,95]. This means that CPX is safe for in vivo use and that much information related to its pharmacodynamics and pharmacokinetics is already well-known [96–98]. The repositioning drug strategy, which consists of proposing new uses for existing drugs [99], is a growing field of research. The implementation of known compounds for new applications saves a considerable amount of time and resources related to the study of the bioavailability, toxicity, and implementation of these compounds [100–102].

Theoretical calculations of ^{19}F NMR chemical shifts were performed to investigate whether the specific interaction of CPX with the hTOPO-IIβ enzyme can be used as a biologic human topoisomerase identifier. Table 2 contains the average of the calculated values for the theoretical ^{19}F NMR shifts in all tested systems. The data show a high similarity between the experimental value and the theoretical value obtained for CPX in the CPX:explicit water system. The low Δδ value indicates that the method and the level of

theory selected are very accurate for this type of calculation [49]. Secondly, the data show that the value obtained in the calculation using the implicit solvation model, CPX:implicit water, is far from the experimental value. It is worth mentioning that results for the system CPX:implicit are similar to values obtained for CPX in a vacuum. Such results indicate that explicit solvation is adequate for representing the solvent effect on CPX. It can also be inferred that the explicit presence of the water molecules in the calculation is important since it creates the proper hydrogen bonding network of water molecules for calculating ^{19}F NMR spectroscopic parameters [103]. As mentioned, the fluorine nucleus has a high sensitivity when compared to the ^{13}C and ^{15}N nuclei, being almost as sensitive as ^{1}H [104]. In this context, although solvent exposure effects can be difficult to observe in nuclei such as ^{13}C and ^{15}N NMR, for the ^{19}F nucleus, solvent-induced isotopic shifts can be as high as 0.25 ppm, offering an efficient way to probe solvent exposure [105].

Table 2. Experimental vs. theoretically computed ^{19}F NMR chemical shifts at the DFT/B3LYP/aug-cc-pVDZ level for a CPX molecule.

System	^{19}F δ_{ppm}	$\Delta\delta_{ppm}$
CPX:aqueous solution (experimental)	−43.70	0.00
CPX:explicit water	−43.54	−0.16
CPX:hTOPO-II	−49.73	6.03
CPX:vacuum	−55.11	11.41
CPX:implicit water	−56.20	12.50

Analysis of the effect on the ^{19}F NMR chemical shifts caused by the interaction of CPX with hTOPO-II β (Table 2 and Figures 5 and 6) shows that there was a variation of 6.03 ppm in relation to the experimental value for CPX in aqueous solution. NMR spectroscopy is a technique extremely sensitive to conformational effects as well as molecular structure effects, both of which can be directly affected by modifications in the chemical environment [106]. Interactions that are able to alter the electronic distribution or even the HOMO-LUMO boundary orbitals can be factors that modify the chemical shift of molecules [107]. Analysis of the figures reveals that the interactions of CPX with hTOPO-II caused a modification in the electronic density (Figure 6) and the frontier orbitals of CPX (Figure 7), which provides a possible explanation for the change in the fluorine chemical shift. This variation in the ^{19}F NMR chemical shift of CPX when it was interacting with the enzyme, represented in Figure 7, can provide important information regarding the occurrence of the ligand in the free form, and in the complexed form with the human topoisomerase-IIβ enzyme. The characteristic signal of CPX when complexed with the enzyme thus constitutes an interesting form of indirect labeling of these proteins, helping to identify their overproduction in the body and, consequently, in cancer cell mapping [8,18,85].

The results of this study lead us to propose CPX as a possible candidate for ^{19}F NMR probing, which can be utilized in cancer diagnosis [29,45]. The application of fluorine probes is advantageous considering that the natural occurrence of fluorine in biological systems is scarce and the signals from ^{19}F NMR spectroscopy will not find any overlapping background signals to compete with the fluorine probes, making the spectra simple and easy to analyze [46,47]. In comparison, the enzyme concentration in tumor cells is higher [10]. Several previous studies have already proven the efficacy of CPX in inhibiting hTOPO-II, leading to the anti-proliferative and cytotoxic activities of this molecule against several malignant cells [74,108]. Accordingly, we can expect that the CPX probe will be efficient and able to reach the desired location. Finally, our study is the first attempt to investigate the use of ^{19}F NMR of CPX as a probe for cancer diagnosis, providing a starting point for further exploration of this new possibility. Additional experimental studies must be carried out in order to obtain more information on the effective implementation of a probe for this purpose.

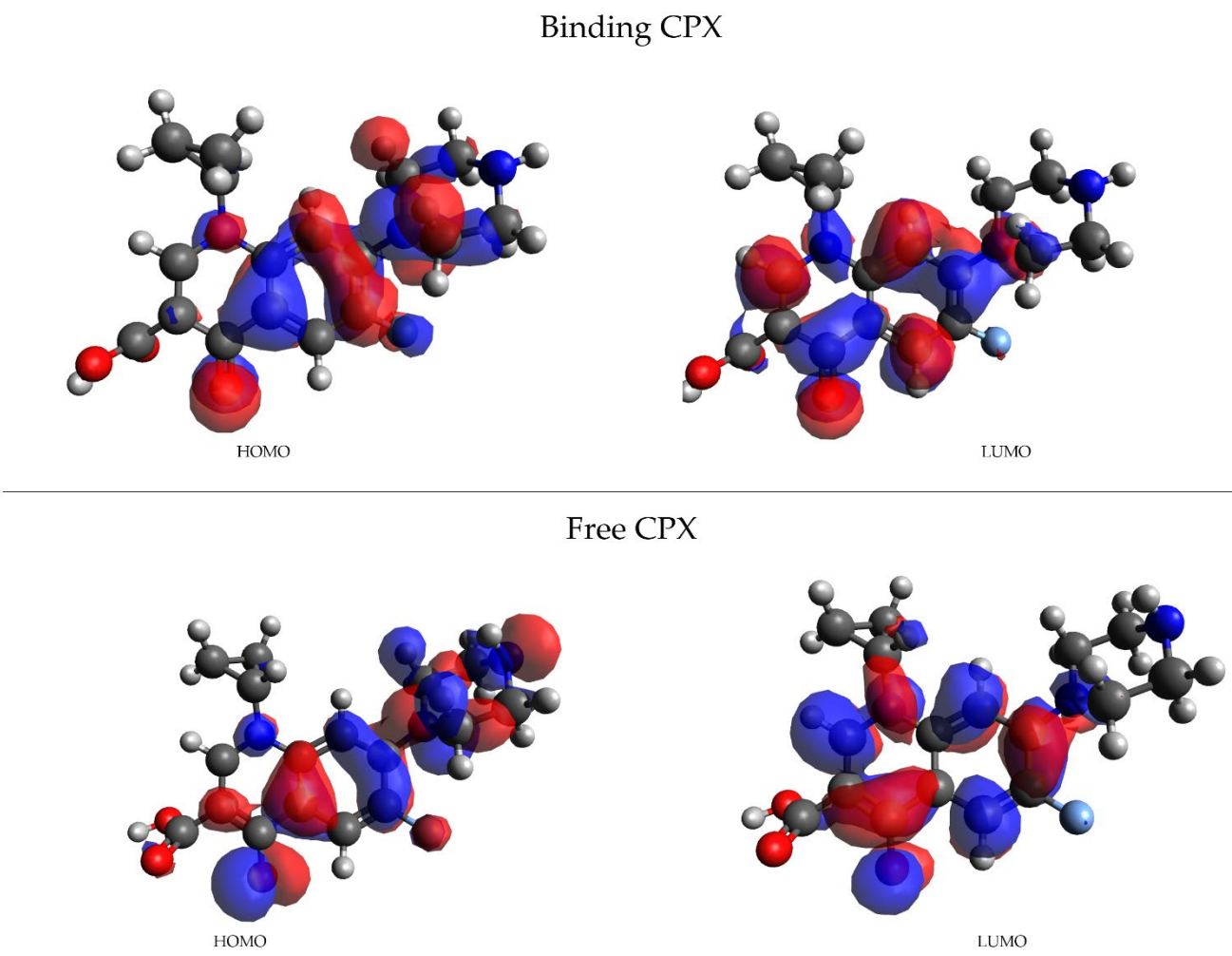

Figure 5. HOMO–LUMO frontier orbital representations for ciprofloxacin molecule in two different environments: in the enzyme active site (binding CPX), and in water (free CPX).

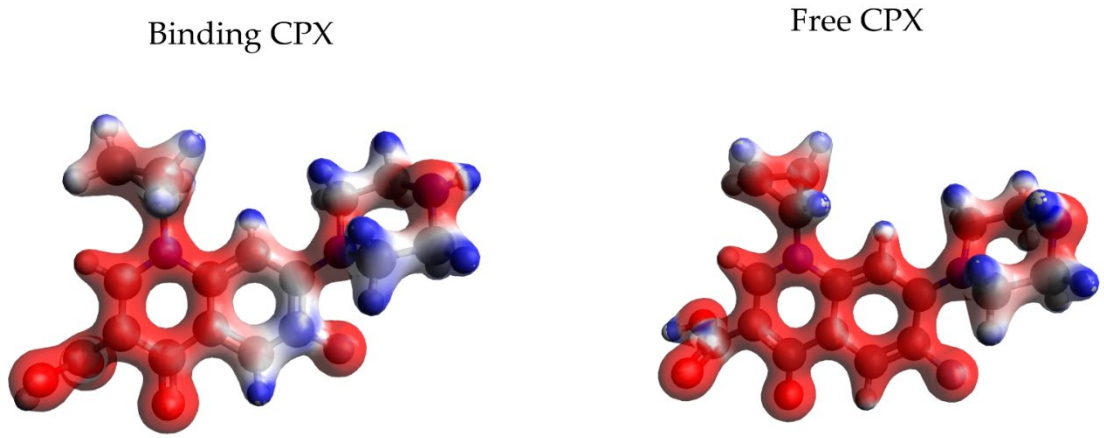

Figure 6. Electronic density variation of ciprofloxacin molecule when binding to the topoisomerase-II enzyme and in a free form in water solvent.

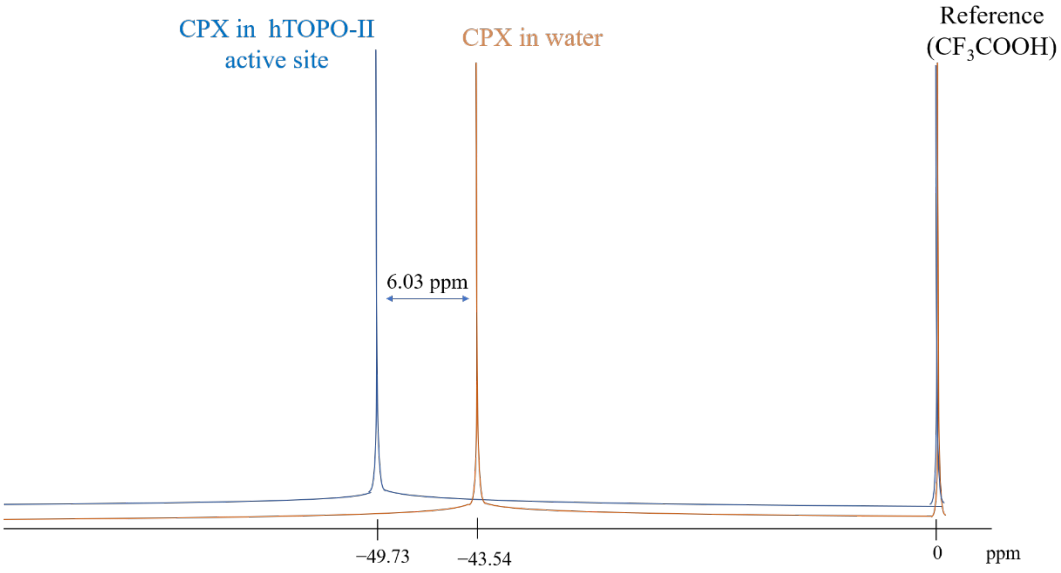

Figure 7. Representation of the variation of the ^{19}F chemical shift for the CPX molecule in the hTOPO-II active site.

4. Conclusions

The results of this study show that the interaction of ciprofloxacin with human topoisomerase-II β can alter the ^{19}F NMR chemical shift signal of ciprofloxacin, when compared to the same parameter for the free molecule in water. Thus, this well-known antimicrobial agent constitutes a possible ^{19}F NMR chemical shift probe for cancer diagnosis, capable of indirectly labeling the overexpression of human topoisomerase-IIβ enzyme in the body, and, consequently, able to assist in the detection of cancer cells.

Considering the results of this study and the low toxicity of this commercially used drug, ciprofloxacin shows promise as an ally in cancer diagnosis. Our results may stimulate new experimental and full-dimensional theoretical investigations that could assess the validity of this assumption. Moreover, our theoretical findings add to the overall understanding of the interaction between ciprofloxacin and the human topoisomerase-II β enzyme and may provide new insights into how it exerts its anti-carcinogenic effect. The results of this study may thus contribute to the development of new tools for cancer diagnosis.

Author Contributions: T.A.S. was responsible for the methodology, planning and execution of experiments, data validation and analysis, and writing. M.A.G. was responsible for the selection of the molecular dynamics structures and for the implementation of the algorithm used in the selections. T.C.R. was responsible for supervision, analysis, visualization, data validation, project and resource management, formal analysis, and writing review. All authors have read and agreed to the published version of the manuscript.

Funding: This work was supported by Conselho Nacional de Desenvolvimento Científico e Tecnológico (CNPq), Fundação de Amparo ao Ensino e Pesquisa de Minas Gerais (FAPEMIG), and Coordenação de Aperfeiçoamento de Pessoal de Nível Superior/Ministério da Defesa (CAPES/MD) (88882.446445/2019-01).

Institutional Review Board Statement: Not applicable.

Informed Consent Statement: Not applicable.

Acknowledgments: The authors wish to thank the Brazilian financial agencies Conselho Nacional de Desenvolvimento Científico e Tecnológico (CNPq), Fundação de Amparo ao Ensino e Pesquisa de Minas Gerais (FAPEMIG), and Coordenação de Aperfeiçoamento de Pessoal de Nível Superior/Ministério da Defesa (CAPES/MD) for financial support, and the Federal University of Lavras (UFLA) and Minas Gerais State University (UEMG) for providing the physical infrastructure.

Conflicts of Interest: Authors declare no conflict of interest.

References

1. Pitman, S.K.; Hoang, U.T.P.; Wi, C.H.; Alsheikh, M.; Hiner, D.A.; Percival, K.M. Revisiting oral fluoroquinolone and multivalent cation drug-drug interactions: Are they still relevant? *Antibiotics* **2019**, *8*, 108. [CrossRef] [PubMed]
2. Qin, P.; Su, B.; Liu, R. Probing the binding of two fluoroquinolones to lysozyme: A combined spectroscopic and docking study. *Mol. Biosyst.* **2012**, *8*, 1222. [CrossRef] [PubMed]
3. Suaifan, G.A.R.Y.; Mohammed, A.A.M. Fluoroquinolones structural and medicinal developments (2013–2018): Where are we now? *Bioorganic Med. Chem.* **2019**, *27*, 3005–3060. [CrossRef] [PubMed]
4. Ali, R.; Alminderej, F.M.; Messaoudi, S.; Saleh, S.M. Ratiometric ultrasensitive optical chemisensor film based antibiotic drug for Al(III) and Cu(II) detection. *Talanta* **2021**, *221*, 121412. [PubMed]
5. Abdel-Aziz, M.; Park, S.E.; Abuo-Rahma, G.E.D.A.A.; Sayed, M.A.; Kwon, Y. Novel N-4-piperazinyl-ciprofloxacin-chalcone hybrids: Synthesis, physicochemical properties, anticancer and topoisomerase I and II inhibitory activity. *Eur. J. Med. Chem.* **2013**, *69*, 427–438. [CrossRef]
6. Majalekar, P.P.; Shirote, P.J. Fluoroquinolones: Blessings or Curses. *Curr. Drug Targets* **2020**, *21*, 1354–1370. [CrossRef]
7. Jacob, D.A.; Mercer, S.L.; Osheroff, N.; Deweese, J.E. Etoposide Quinone Is a Redox-Dependent Topoisomerase II Poison. *Biochemistry* **2011**, *50*, 5660–5667. [CrossRef]
8. Idowu, T.; Schweizer, F. Ubiquitous nature of fluoroquinolones: The oscillation between antibacterial and anticancer activities. *Antibiotics* **2017**, *6*, 26. [CrossRef]
9. Bisacchi, G.; Hale, M. A "Double-Edged" Scaffold: Antitumor Power within the Antibacterial Quinolone. *Curr. Med. Chem.* **2016**, *23*, 520–577. [CrossRef]
10. Heestand, G.M.; Schwaederle, M.; Gatalica, Z.; Arguello, D.; Kurzrock, R. Topoisomerase expression and amplification in solid tumours: Analysis of 24,262 patients. *Eur. J. Cancer* **2017**, *83*, 80–87. [CrossRef]
11. Suresh, N.; Suresh, A.; Yerramsetty, S.; Bhadra, M.P.; Alvala, M.; Sekhar, K.V.G.C. Anti-proliferative activity, molecular modeling studies and interaction with calf thymus DNA of novel ciprofloxacin analogues. *J. Chem. Sci.* **2018**, *130*, 1–11. [CrossRef]
12. Beberok, A.; Wrześniok, D.; Rok, J.; Rzepka, Z.; Respondek, M.; Buszman, E. Ciprofloxacin triggers the apoptosis of human triple-negative breast cancer MDA-MB-231 cells via the p53/Bax/Bcl-2 signaling pathway. *Int. J. Oncol.* **2018**, *52*, 1727–1737. [CrossRef] [PubMed]
13. Chekerov, R.; Klaman, I.; Zafrakas, M.; Könsgen, D.; Mustea, A.; Petschke, B.; Lichtenegger, W.; Sehouli, J.; Dahl, E. Altered Expression Pattern of Topoisomerase IIα in Ovarian Tumor Epithelial and Stromal Cells after Platinum-Based Chemotherapy. *Neoplasia* **2006**, *8*, 38. [CrossRef] [PubMed]
14. Faggad, A.; Darb-Esfahani, S.; Wirtz, R.; Sinn, B.; Sehouli, J.; Könsgen, D.; Lage, H.; Weichert, W.; Noske, A.; Budczies, J.; et al. Topoisomerase IIα mRNA and protein expression in ovarian carcinoma: Correlation with clinicopathological factors and prognosis. *Mod. Pathol.* **2009**, *22*, 579–588. [CrossRef] [PubMed]
15. Bai, Y.; Li, L.D.; Li, J.; Lu, X. Targeting of topoisomerases for prognosis and drug resistance in ovarian cancer. *J. Ovarian Res.* **2016**, *9*, 1–12. [CrossRef] [PubMed]
16. Zhou, H.; Tang, J.; Zhang, J.; Chen, B.; Kan, J.; Zhang, W.; Zhou, J.; Ma, H. A red lysosome-targeted fluorescent probe for carboxylesterase detection and bioimaging. *J. Mater. Chem. B* **2019**, *7*, 2989–2996. [CrossRef]
17. Kirk, E.; Hevenern, T.A.; Verstak, K.E.L.; Daniel, L.; Riggsbee, J.W.M. Recent developments in topoisomerase-targeted cancer chemotherapy. *Acta Pharm. Sin. B* **2018**, *8*, 844–861.
18. Cinelli, M.A. Topoisomerase 1B poisons: Over a half-century of drug leads, clinical candidates, and serendipitous discoveries. *Med. Res. Rev.* **2019**, *39*, 1294–1337. [CrossRef]
19. Verma, A. Prions, prion-like prionoids, and neurodegenerative disorders. *Ann. Indian Acad. Neurol.* **2016**, *19*, 169–174. [CrossRef]
20. Pilleron, S.; Soto-Perez-de-Celis, E.; Vignat, J.; Ferlay, J.; Soerjomataram, I.; Bray, F.; Sarfati, D. Estimated global cancer incidence in the oldest adults in 2018 and projections to 2050. *Int. J. Cancer* **2021**, *148*, 601–608. [CrossRef]
21. Dan, N.; Setua, S.; Kashyap, V.; Khan, S.; Jaggi, M.; Yallapu, M.; Chauhan, S.; Dan, N.; Setua, S.; Kashyap, V.K.; et al. Antibody-Drug Conjugates for Cancer Therapy: Chemistry to Clinical Implications. *Pharmaceuticals* **2018**, *11*, 32. [CrossRef] [PubMed]
22. Bray, F.; Ferlay, J.; Soerjomataram, I.; Siegel, R.L.; Torre, L.A.; Jemal, A. Global cancer statistics 2018: GLOBOCAN estimates of incidence and mortality worldwide for 36 cancers in 185 countries. *Cancer J. Clin.* **2018**, *68*, 394–424. [CrossRef]
23. Kassab, A.E.; Gedawy, E.M. Novel ciprofloxacin hybrids using biology oriented drug synthesis (BIODS) approach: Anticancer activity, effects on cell cycle profile, caspase-3 mediated apoptosis, topoisomerase II inhibition, and antibacterial activity. *Eur. J. Med. Chem.* **2018**, *150*, 403–418. [CrossRef] [PubMed]
24. Pashayan, N.; Pharoah, P.D.P. The challenge of early detection in cancer. *Science* **2020**, *368*, 589–590. [CrossRef] [PubMed]
25. Holtedahl, K. Challenges in early diagnosis of cancer: The fast track. *Scand. J. Prim. Health Care* **2020**, *38*, 251–252. [CrossRef] [PubMed]
26. World Health Organization. Module 3: Early Detection. *Cancer Control: Knowledge into Action: WHO Guide for Effective Programmes* **2007**, 1–50. [PubMed]
27. Unger-Saldaña, K. Challenges to the early diagnosis and treatment of breast cancer in developing countries. *World J. Clin. Oncol.* **2014**, *5*, 465. [CrossRef] [PubMed]

28. Lue, N.; Kang, J.W.; Yu, C.-C.; Barman, I.; Dingari, N.C.; Feld, M.S.; Dasari, R.R.; Fitzmaurice, M. Portable Optical Fiber Probe-Based Spectroscopic Scanner for Rapid Cancer Diagnosis: A New Tool for Intraoperative Margin Assessment. *PLoS ONE* **2012**, *7*, e30887. [CrossRef]
29. Pereira, B.T.L.L.; Gonçalves, M.A.; Mancini, D.T.; Kuca, K.; Ramalho, T.C. First attempts of the use of 195Pt NMR of phenylbenzothiazole complexes as spectroscopic technique for the cancer diagnosis. *Molecules* **2019**, *24*, 3970. [CrossRef]
30. da Rocha, E.P.; Rodrigues, H.A.; da Cunha, E.F.F.; Ramalho, T.C. Probing kinetic and thermodynamic parameters as well as solvent and substituent effects on spectroscopic probes of 2-amino-1,4-naphthoquinone derivatives. *Comput. Theor. Chem.* **2016**, *1096*, 17–26. [CrossRef]
31. Wan, X.; Wang, H.; Shi, B.; Guo, Y.; Liu, S.Y.; Wang, X. An enzyme activated fluorescent probe for LTA4H activity sensing and its application in cancer screening. *Talanta* **2023**, *253*, 123887. [CrossRef]
32. Zhou, X.; Bai, D.; Yu, H.; Fu, Y.; Song, L.; Wu, Y.; Chen, K.; Li, J.; Yang, Y.; Chen, H.; et al. Detection of rare CTCs by electrochemical biosensor built on quaternary PdPtCuRu nanospheres with mesoporous architectures. *Talanta* **2023**, *253*, 123955. [CrossRef] [PubMed]
33. Gab, M.; Allah, A.; Sarhan, M.A.; Elshennawy, M.N. Edge U-Net: Brain tumor segmentation using MRI based on deep U-Net model with boundary information. *Expert Syst. Appl.* **2023**, *213*, 118833.
34. Kim, J.H.; An, Y.J.; Kim, T.M.; Kim, J.E.; Park, S.; Choi, S.H. Ex vivo NMR metabolomics approach using cerebrospinal fluid for the diagnosis of primary CNS lymphoma: Correlation with MR imaging characteristics. *Cancer Med.* **2022**, *00*, 1–11. [CrossRef] [PubMed]
35. Saleem, H.; Maryam, A.; Bokhari, S.A.; Ashiq, A.; Rauf, S.A.; Khalid, R.R.; Qureshi, F.A.; Siddiqi, A.R. Design, synthesis, characterization and computational docking studies of novel sulfonamide derivatives. *EXCLI J.* **2018**, *17*, 169–180.
36. Larkin, J.R.; Anthony, S.; Johanssen, V.A.; Yeo, T.; Sealey, M.; Yates, A.G.; Smith, C.F.; Claridge, T.D.W.; Nicholson, B.D.; Moreland, J.A.; et al. Metabolomic Biomarkers in Blood Samples Identify Cancers in a Mixed Population of Patients with Nonspecific Symptoms. *Clin. Cancer Res.* **2022**, *28*, 1651–1661. [CrossRef]
37. Derveauex, E.; Thomeer, M.; Mesotten, L.; Reekmans, G.; Adriaensens, P. Detection of Lung Cancer via Blood Plasma and 1H-NMR Metabolomics: Validation by a Semi-Targeted and Quantitative Approach Using a Protein-Binding Competitor. *Metabolites* **2021**, *11*, 537. [CrossRef] [PubMed]
38. Kwon, H.N.; Lee, H.; Park, J.W.; Kim, Y.H.; Park, S.; Kim, J.J. Screening for Early Gastric Cancer Using a Noninvasive Urine Metabolomics Approach. *Cancers* **2020**, *12*, 2904. [CrossRef]
39. Michálková, L.; Horník, Š.; Sýkora, J.; Habartová, L.; Setnička, V. Diagnosis of pancreatic cancer via1H NMR metabolomics of human plasma. *Analyst* **2018**, *143*, 5974–5978. [CrossRef]
40. Mikkonen, J.J.W.; Singh, S.P.; Akhi, R.; Salo, T.; Lappalainen, R.; González-Arriagada, W.A.; Lopes, M.A.; Kullaa, A.M.; Myllymaa, S. Potential role of nuclear magnetic resonance spectroscopy to identify salivary metabolite alterations in patients with head and neck cancer. *Oncol. Lett.* **2018**, *16*, 6795–6800. [CrossRef]
41. Erben, V.; Bhardwaj, M.; Schrotz-King, P.; Brenner, H. Metabolomics Biomarkers for Detection of Colorectal Neoplasms: A Systematic Review. *Cancers* **2018**, *10*, 246. [CrossRef] [PubMed]
42. Yang, B.; Liao, G.; Wen, X.; Chen, W.; Cheng, S.; Stolzenburg, J.U.; Ganzer, R.; Neuhaus, J. Nuclear magnetic resonance spectroscopy as a new approach for improvement of early diagnosis and risk stratification of prostate cancer. *J. Zhejiang Univ. B* **2017**, *18*, 921–933. [CrossRef] [PubMed]
43. Tang, Z.-Y.; Zhang, Y.; Chen, Y.-T.; Yu, Q.; An, L.-K. The first small fluorescent probe as Tyrosyl-DNA phosphodiesterase 1 (TDP1) substrate. *Dye. Pigment.* **2019**, *169*, 45–50. [CrossRef]
44. Zhou, J.; Ma, H. Design principles of spectroscopic probes for biological applications. *Chem. Sci.* **2016**, *7*, 6309–6315. [CrossRef] [PubMed]
45. Stanley, P.D. Principles and Topical Applications of 19F NMR Spectrometry. In *Organofluorines. The Handbook of Environmental Chemistry*; Neilson, A.H., Ed.; Springer: Berlin/Heidelberg, Germany, 2002; Volume 3N, pp. 1–61.
46. .Marsh, E.N.G.; Suzuki, Y. Using ^{19}F NMR to Probe Biological Interactions of Proteins and Peptides. *ACS Chem. Biol.* **2014**, *9*, 1242–1250. [CrossRef]
47. Gimenez, D.; Phelan, A.; Murphy, C.D.; Cobb, S.L. ^{19}F NMR as a tool in chemical biology. *Beilstein J. Org. Chem.* **2021**, *17*, 293–318. [CrossRef] [PubMed]
48. Jawaria, R.; Hussain, M.; Khalid, M.; Khan, M.U.; Tahir, M.N.; Naseer, M.M.; Braga, A.A.C.; Shafiq, Z. Synthesis, crystal structure analysis, spectral characterization and nonlinear optical exploration of potent thiosemicarbazones based compounds: A DFT refine experimental study. *Inorg. Chim. Acta* **2019**, *486*, 162–171. [CrossRef]
49. Koch, A.; Stamboliyska, B.; Mikhova, B.; Breznica-Selmani, P.; Mladenovska, K.; Popovski, E. Calculations of 13C NMR chemical shifts and F–C coupling constants of ciprofloxacin. *Magn. Reson. Chem.* **2019**, *57*, S75–S84. [CrossRef]
50. Ghosh, D.; Rhodes, S.; Winder, D.; Atkinson, A.; Gibson, J.; Ming, W.; Padgett, C.; Landge, S.; Aiken, K. Spectroscopic investigation of bis-appended 1,2,3-triazole probe for the detection of Cu(II) ion. *J. Mol. Struct.* **2017**, *1134*, 638–648. [CrossRef]
51. Ramalho, T.C.; Taft, C.A. Thermal and solvent effects on the NMR and UV parameters of some bioreductive drugs. *J. Chem. Phys.* **2005**, *123*, 054319. [CrossRef]

52. Pudipeddi, A.; Vasudevan, S.; Shanmugam, K.; Mohan, S.S.; Vairaprakash, P.; Neelakantan, P.; Balraj, A.S.; Solomon, A.P. Design, dynamic docking, synthesis, and in vitro validation of a novel DNA gyrase B inhibitor. *J. Biomol. Struct. Dyn.* **2022**, *4*, 1–14. [CrossRef] [PubMed]
53. Khan, T.; Sankhe, K.; Suvarna, V.; Sherje, A.; Patel, K.; Dravyakar, B. DNA gyrase inhibitors: Progress and synthesis of potent compounds as antibacterial agents. *Biomed. Pharmacother.* **2018**, *103*, 923–938. [CrossRef] [PubMed]
54. Berman, H.M.; Westbrook, J.; Feng, Z.; Gilliland, G.; Bhat, T.N.; Weissig, H.; Shindyalov, I.N.; Bourne, P.E. The Protein Data Bank. *Nucleic Acids Res.* **2000**, *28*, 235–242. [CrossRef] [PubMed]
55. Malde, A.K.; Zuo, L.; Breeze, M.; Stroet, M.; Poger, D.; Nair, P.C.; Oostenbrink, C.; Mark, A.E. An Automated force field Topology Builder (ATB) and repository: Version 1.0. *J. Chem. Theory Comput.* **2011**, *7*, 4026–4037. [CrossRef] [PubMed]
56. Abraham, M.J.; Murtola, T.; Schulz, R.; Páll, S.; Smith, J.C.; Hess, B.; Lindah, E. Gromacs: High performance molecular simulations through multi-level parallelism from laptops to supercomputers. *SoftwareX* **2015**, *1–2*, 19–25. [CrossRef]
57. Christen, M.; Hünenberger, P.H.; Bakowies, D.; Baron, R.; Bürgi, R.; Geerke, D.P.; Heinz, T.N.; Kastenholz, M.A.; Kräutler, V.; Oostenbrink, C.; et al. The GROMOS software for biomolecular simulation: GROMOS05. *J. Comput. Chem.* **2005**, *26*, 1719–1751. [CrossRef]
58. Gonçalves, M.A.; Santos, L.S.; Prata, D.M.; Peixoto, F.C.; da Cunha, E.F.F.; Ramalho, T.C. Optimal wavelet signal compression as an efficient alternative to investigate molecular dynamics simulations: Application to thermal and solvent effects of MRI probes. *Theor. Chem. Acc.* **2017**, *136*, 15. [CrossRef]
59. Frisch, M.J.; Trucks, G.W.; Schlegel, H.B.; Scuseria, G.E.; Robb, M.A.; Cheeseman, J.R.; Scalmani, G.; Barone, V.; Mennucci, B.; Petersson, G.A.; et al. *Gaussian 09*; Gaussian, Inc.: Wallingford, CT, USA, 2009.
60. Dunning, T.H., Jr. Gaussian basis sets for use in correlated molecular calculations. I. The atoms boron through neon and hydrogen. *J. Chem. Phys.* **1998**, *90*, 1007. [CrossRef]
61. Kendall, R.A.; Dunning, T.H., Jr.; Harrison, R.J. Electron affinities of the first-row atoms revisited. Systematic basis sets and wave functions. *J. Chem. Phys.* **1998**, *96*, 6796. [CrossRef]
62. Woon, D.E., Jr. Gaussian basis sets for use in correlated molecular calculations. III. The atoms aluminum through argon. *J. Chem. Phys.* **1998**, *98*, 1358. [CrossRef]
63. Wolinski, K.; Hinton, J.F.; Pulay, P. Efficient implementation of the gauge-independent atomic orbital method for NMR chemical shift calculations. *J. Am. Chem. Soc.* **2002**, *112*, 8251–8260. [CrossRef]
64. Mejía-Urueta, R.; Mestre-Quintero, K.; Vivas-Reyes, R. DFT-GIAO Calculation of Properties of 19 F NMR and Stability Study of Environmentally Relevant Perfluoroalkylsulfonamides (PFASAmide). *Artic. J. Braz. Chem. Soc.* **2011**, *22*, 2268–2274.
65. Dapprich, S.; Komáromi, I.; Byun, K.S.; Morokuma, K.; Frisch, M.J. A new ONIOM implementation in Gaussian98. Part I. The calculation of energies, gradients, vibrational frequencies and electric field derivatives. *J. Mol. Struct. Theochem.* **1999**, *461–462*, 1–21. [CrossRef]
66. Marenich, A.V.; Cramer, C.J.; Truhlar, D.G. Universal Solvation Model Based on Solute Electron Density and on a Continuum Model of the Solvent Defined by the Bulk Dielectric Constant and Atomic Surface Tensions. *J. Phys. Chem. B* **2009**, *113*, 6378–6396. [CrossRef]
67. Trefi, S.; Gilard, V.; Malet-Martino, M.; Martino, R. Generic ciprofloxacin tablets contain the stated amount of drug and different impurity profiles: A ^{19}F, 1H and DOSY NMR analysis. *J. Pharm. Biomed. Anal.* **2007**, *44*, 743–754. [CrossRef]
68. Zhang, F.-F.; Jiang, M.-H.; Sun, L.-L.; Zheng, F.; Dong, L.; Shah, V.; Shen, W.-B.; Ding, Y. Quantitative analysis of sitagliptin using the ^{19}F-NMR method: A universal technique for fluorinated compound detection. *Analyst* **2015**, *140*, 280–286. [CrossRef]
69. Ezelarab, H.A.A.; Abbas, S.H.; Hassan, H.A.; Abuo-Rahma, G.E.D.A. Recent updates of fluoroquinolones as antibacterial agents. *Arch. Pharm.* **2018**, *351*, 1800141. [CrossRef]
70. Fief, C.A.; Hoang, K.G.; Phipps, S.D.; Wallace, J.L.; Deweese, J.E. Examining the Impact of Antimicrobial Fluoroquinolones on Human DNA Topoisomerase IIα and IIβ. *ACS Omega* **2019**, *4*, 4049–4055. [CrossRef]
71. Beberok, A.; Wrześniok, D.; Minecka, A.; Rok, J.; Delijewski, M.; Rzepka, Z.; Respondek, M.; Buszman, E. Ciprofloxacin-mediated induction of S-phase cell cycle arrest and apoptosis in COLO829 melanoma cells. *Pharmacol. Rep.* **2018**, *70*, 6–13. [CrossRef]
72. Perrone, C.E.; Takahashi, K.C.; Williams, G.M. Inhibition of human topoisomerase IIα by fluoroquinolones and ultraviolet A irradiation. *Toxicol. Sci.* **2002**, *69*, 16–22. [CrossRef]
73. Swedan, H.K.; Kassab, A.E.; Gedawy, E.M.; Elmeligie, S.E. Design, synthesis, and biological evaluation of novel ciprofloxacin derivatives as potential anticancer agents targeting topoisomerase II enzyme. *J. Enzym. Inhib. Med. Chem.* **2023**, *38*, 118–137. [CrossRef] [PubMed]
74. Mazandaran, K.E.; Mirshokraee, S.A.; Didehban, K.; Houshdar Tehrani, M.H. Design, Synthesis and Biological Evaluation of Ciprofloxacin- Peptide Conjugates as Anticancer Agents. *Iran. J. Pharm. Res. IJPR* **2019**, *18*, 1823.
75. Mohammed, H.H.H.; Abd El-Hafeez, A.A.; Ebeid, K.; Mekkawy, A.I.; Abourehab, M.A.S.; Wafa, E.I.; Alhaj-Suliman, S.O.; Salem, A.K.; Ghosh, P.; Abuo-Rahma, G.E.D.A.; et al. New 1,2,3-triazole linked ciprofloxacin-chalcones induce DNA damage by inhibiting human topoisomerase I& II and tubulin polymerization. *J. Enzym. Inhib. Med. Chem.* **2022**, *37*, 1346–1363.
76. Mohammed, H.H.H.; Abbas, S.H.; Hayallah, A.M.; Abuo-Rahma, G.E.D.A.; Mostafa, Y.A. Novel urea linked ciprofloxacin-chalcone hybrids having antiproliferative topoisomerases I/II inhibitory activities and caspases-mediated apoptosis. *Bioorg. Chem.* **2021**, *106*, 104422. [CrossRef]

77. Sales, T.A.; Ramalho, T.C. Ciprofloxacin/Topoisomerase-II complex as a promising dual UV–Vis/fluorescent probe: Accomplishments and opportunities for the cancer diagnosis. *Theor. Chem. Acc.* **2022**, *141*, 1–10. [CrossRef]
78. Cowen, T.; Karim, K.; Piletsky, S. No Title. *Anal. Chim. Acta* **2016**, *936*, 62–74. [CrossRef]
79. Jadhav, A.K.; Karuppayil, S.M. Molecular docking studies on thirteen fluoroquinolines with human topoisomerase II a and b. *Silico Pharmacol.* **2017**, *5*, 1–12. [CrossRef] [PubMed]
80. Patel, J.R.; Joshi, H.V.; Shah, U.A.; Patel, J.K. A Review on Computational Software Tools for Drug Design and Discovery. *Indo. Glob. J. Pharm. Sci.* **2022**, *12*, 53–81. [CrossRef]
81. Pajeva, I.; Tsakovska, I.; Pencheva, T.; Alov, P.; Al Sharif, M.; Lessigiarska, I.; Jereva, D.; Diukendjieva, A. In silico Studies of Biologically Active Molecules. *Stud. Comput. Intell.* **2021**, *934*, 421–451.
82. Caballero, J. The latest automated docking technologies for novel drug discovery. *Expert Opin. Drug Discov.* **2020**, *16*, 625–645. [CrossRef] [PubMed]
83. Frye, L.; Bhat, S.; Akinsanya, K.; Abel, R. From computer-aided drug discovery to computer-driven drug discovery. *Drug Discov. Today Technol.* **2021**, *39*, 111–117. [CrossRef] [PubMed]
84. Shukla, R.; Tripathi, T. Molecular Dynamics Simulation in Drug Discovery: Opportunities and Challenges. In *Innovations and Implementations of Computer Aided Drug Discovery Strategies in Rational Drug Design*; Singh, S.K.., Ed.; Springer: Singapore, 2021; pp. 295–316.
85. McClendon, A.K.; Osheroff, N. DNA Topoisomerase II, Genotoxicity, and Cancer. *Mutat. Res. Mol. Mech. Mutagen.* **2007**, *623*, 83–97. [CrossRef] [PubMed]
86. Sales, T.A.; Marcussi, S.; da Cunha, E.F.F.; Kuca, K.; Ramalho, T.C. Can inhibitors of snake venom phospholipases A_2 lead to new insights into anti-inflammatory therapy in humans? A theoretical study. *Toxins* **2017**, *9*, 341. [CrossRef] [PubMed]
87. Schreiner, W.; Karch, R.; Knapp, B.; Ilieva, N. Relaxation estimation of RMSD in molecular dynamics immunosimulations. *Comput. Math. Methods Med.* **2012**, *2012*, 173521. [CrossRef] [PubMed]
88. Bhardwaj, P.; Biswas, G.P.; Mahata, N.; Ghanta, S.; Bhunia, B. Exploration of binding mechanism of triclosan towards cancer markers using molecular docking and molecular dynamics. *Chemosphere* **2022**, *293*, 133550. [CrossRef]
89. Chekmenev, E.Y.; Chow, S.K.; Tofan, D.; Weitekamp, D.P.; Ross, B.D.; Bhattacharya, P. Fluorine-19 NMR chemical shift probes molecular binding to lipid membranes. *J. Phys. Chem. B* **2008**, *112*, 6285–6287. [CrossRef] [PubMed]
90. Maxwell, R.J.; Workman, P.; Griffiths, J.R. Demonstration of tumor-selective retention of fluorinated nitroimidazole probes by ^{19}F magnetic resonance spectroscopy in vivo. *Int. J. Radiat. Oncol.* **1989**, *16*, 925–929. [CrossRef] [PubMed]
91. Peterson, K.L.; Srivastava, K.; Pierre, V.C. Fluorinated paramagnetic complexes: Sensitive and responsive probes for magnetic resonance spectroscopy and imaging. *Front. Chem.* **2018**, *6*, 160. [CrossRef] [PubMed]
92. Ojugo, A.S.E.; Mcsheehy, P.M.J.; Mcintyre, D.J.O.; Mccoy, C.; Stubbs, M.; Leach, M.O.; Judson, I.R.; Grifths, J.R. Measurement of the extracellular pH of solid tumours in mice by magnetic resonance spectroscopy: A comparison of exogenous 19 F and 31 P probes. *NMR Biomed. Int. J. Devoted Dev. Appl. Magn. Reson. Vivo* **1999**, *12*, 495–504.
93. Ye, Y.; Liu, X.; Zhang, Z.; Wu, Q.; Jiang, B.; Jiang, L.; Zhang, X.; Liu, M.; Pielak, G.J.; Li, C. ^{19}FNMR Spectroscopy as a Probe of Cytoplasmic Viscosity and Weak Protein Interactions in Living Cells. *Chem. A Eur. J.* **2013**, *19*, 12705–12710. [CrossRef]
94. Ulrich, A.S. Solid state ^{19}F NMR methods for studying biomembranes. *Prog. Nucl. Magn. Reson. Spectrosc.* **2005**, *46*, 1–21. [CrossRef]
95. Centers for Disease Control and Prevention. *Outpatient Antibiotic Prescriptions—United States*; CDC: Atlanta, GA, USA, 2017.
96. Crump, B.; Wise, R.; Dent, J. Pharmacokinetics and tissue penetration of ciprofloxacin. *Antimicrob. Agents Chemother.* **1983**, *24*, 784–786. [CrossRef] [PubMed]
97. Brunner, M.; Staß, H.; Möller, J.G.; Schrolnberger, C.; Erovic, B.; Hollenstein, U.; Zeitlinger, M.; Georg Eichler, H.; Müller, M. Target Site Concentrations of Ciprofloxacin after Single Intravenous and Oral Doses. *Antimicrob. Agents Chemother.* **2002**, *46*, 3724. [CrossRef] [PubMed]
98. Yuan, F.; Hu, C.; Hu, X.; Wei, D.; Chen, Y.; Qu, J. Photodegradation and toxicity changes of antibiotics in UV and UV/H_2O_2 process. *J. Hazard. Mater.* **2011**, *185*, 1256–1263. [CrossRef]
99. Ashburn, T.T.; Thor, K.B. Drug repositioning: Identifying and developing new uses for existing drugs. *Nat. Rev. Drug Discov.* **2004**, *3*, 673–683. [CrossRef]
100. Mucke, H.A. The case of galantamine: Repurposing and late blooming of a cholinergic drug. *Futur. Sci. OA* **2015**, *1*. [CrossRef]
101. Mullard, A. Drug repurposing programmes get lift off. *Nat. Rev. Drug Discov.* **2012**, *11*, 505–506. [CrossRef]
102. Durães, F.; Pinto, M.; Sousa, E.; Durães, F.; Pinto, M.; Sousa, E. Old Drugs as New Treatments for Neurodegenerative Diseases. *Pharmaceuticals* **2018**, *11*, 44. [CrossRef]
103. Edmond, L.Y.; Gerig, J.T. Origins of Fluorine NMR Chemical Shifts in Fluorine-Containing Proteins. *J. Am. Chem. Soc.* **2000**, *122*, 4408–4417.
104. Modo, M. ^{19}F Magnetic Resonance Imaging and Spectroscopy in Neuroscience. *Neuroscience* **2021**, *474*, 37–50. [CrossRef]
105. Evanics, F.; Kitevski, J.L.; Bezsonova, I.; Forman-Kay, J.; Prosser, R.S. ^{19}F NMR studies of solvent exposure and peptide binding to an SH3 domain. *Biochim. Biophys. Acta Gen. Subj.* **2007**, *1770*, 221–230. [CrossRef] [PubMed]
106. Gonçalves, M.A.; Gonçalves, A.S.; Franca, T.C.C.; Santana, M.S.; da Cunha, E.F.F.; Ramalho, T.C. Improved Protocol for the Selection of Structures from Molecular Dynamics of Organic Systems in Solution: The Value of Investigating Different Wavelet Families. *J. Chem. Theory Comput.* **2022**, *18*, 5810–5818. [CrossRef] [PubMed]

107. Rayene, K.; Imane, D.; Abdelaziz, B.; Leila, N.; Fatiha, M.; Abdelkrim, G.; Bouzid, G.; Ismahan, L.; Brahim, H.; Rabah, O. Molecular modeling study of structures, Hirschfield surface, NBO, AIM, RDG, IGM and 1HNMR of thymoquinone/hydroxypropyl-β-cyclodextrin inclusion complex from QM calculations. *J. Mol. Struct.* **2022**, *1249*, 131565. [CrossRef]
108. Jaber, D.F.; Jallad, M.A.N.; Abdelnoor, A.M. The effect of ciprofloxacin on the growth of B16F10 melanoma cells. *J. Cancer Res. Ther.* **2017**, *13*, 956–960. [PubMed]